

Numerical Modeling of Supercritical ‘Out-Salting’ in the ‘Atlantis II Deep’ (Red Sea) Hydrothermal System

Martin Hovland^{*1}, Håkon Rueslåtten², Tatyana Kutznetsova³, Bjørn Kvamme³, Gunnar E. Fladmark⁴ and Hans Konrad Johnsen⁵

¹ Statoil, N-4035, Stavanger, Norway

² NumericalRocks, N-7000, Trondheim, Norway

³ Department of Physics and Technology, University of Bergen, N-5000 Bergen, Norway

⁴ Department of Mathematics, University of Bergen, N-5000 Bergen, Norway

⁵ Statoil, R&D Department, Rotvoll, N-7000 Trondheim, Norway

Abstract: Supercritical water behaves close to that of a non-polar fluid and its ability to dissolve salt ions is very low. In rifting locations world-wide, where hot vents occur, it has been shown that seawater attains supercritical conditions. We therefore anticipate that circulation of seawater in hydrothermal systems passing through regions of the supercritical domain results in spontaneous precipitation of salt particles. Thus, the hot ‘geysers’ of saturated brines observed in the ‘Atlantis II Deep’ of the Red Sea could result from re-dissolution of salts accumulated in underground fracture systems. Here we report on an advanced numerical modeling study which demonstrates, for the first time, that there is a forced convection cell where salts precipitate and accumulate. These combined numerical thermodynamic simulations and basin modeling results also demonstrate that hot brines reflux back to surface immediately above the magma chamber located beneath the axis of the rift. Based on this study, we predict that hydrothermal ‘out-salting’ is the main cause of dense, warm brines accumulating in the central portion of the Red Sea. Furthermore, the results are relevant for understanding how large volumes of evaporites (salts) accumulate along rifted plate margins.

Keywords: Supercritical out-salting, hydrothermal system, brine, salts, magma chamber, Atlantis II Deep, Red Sea.

INTRODUCTION

Laboratory experiments and industrial practice have demonstrated that solid salts precipitate from seawater and brines when the fluids pass beyond their supercritical P-T points on the boiling curve [1-3]. The process was first named ‘shock crystallization’, but we prefer the term hydrothermal ‘out-salting’ [2, 4]. Physico-chemically, this occurs because supercritical water behaves like a non-polar, low density fluid. In contrast to ‘normal’ liquid water, supercritical water loses its ability to dissolve salts in a certain P-T window [3]. The complete P-T window of very low solubility stretches beyond the supercritical region into the gas region. But what is special about the supercritical region close to the critical point is the combination of high molecular mobility and fairly high density compared to gas density, which increases the rates of nucleation and solid salt crystal growth dramatically [5]. Numerically, such phase transitions and out-salting regimes can be handled and modeled by molecular simulations, like we have demonstrated herein [4, 6].

GEOLOGICAL SETTING/BASIS FOR MODELING

Up to 5 km thick deposits of bedded salts (evaporites), believed to have formed during the last 5 million years [7] are found on the flanks of the central Red Sea [8, 9]. In a study of active hydrothermal processes of the Atlantis II

Deep, Ramboz *et al.* [10] found evidence of boiling brines and geyser-type discharges on the seafloor at a water depth of 2,050 m. Liquid inclusions with up to ~33 wt % salts (NaCl equivalents) were also encountered: “Near-isothermal long-duration boiling of solutions implies a deep fluid reservoir with a limited volume, and heated by magma. The salt-enriched liquids were injected intermittently on the seafloor, and then cooled without mixing” [10].

In 1974, the Deep Sea Drilling Project (DSDP) attempted drilling into the shallow basalt located below the Atlantis II Deep. The drilling team encountered very difficult drilling and sampling conditions and only managed to penetrate 14 m into the seafloor. The two cores obtained, contained Late Quaternary sediments: mixed montmorillonite, anhydrite (salt), and goethite-hematite facies in the upper 5 m with fresh basalt fragments in the lower 9 m [11].

Prior to the drilling, three pools of hot brines ($\leq 70^\circ\text{C}$) were found within the Atlantis II Deep [9]. The sediments underlying these brines are enriched in heavy metals (e.g. Cu, Pb, Zn, Ag, and Au). At another drilling site (DSDP Site 225) located 16 km to the east of the Atlantis II Deep, at 1,228 m water depth, the drill penetrated 230 m and terminated 54 m into the Late Miocene evaporite (salt) sequence. The deeper sedimentary units consist of anhydrite and halite inter-bedded with black shales [12]. The dark muds and shales above the evaporite sequence are occasionally enriched with Fe, V ($\leq 1,000$ ppm), and Mo (≤ 500 ppm), indicating a hydrothermal origin.

*Address correspondence to this author at Statoil, N-4035, Stavanger, Norway; E-mail: MHOVLAND@statoil.com

Oceanic Crust and Circulation of Fluids

Extensive studies of buried hydrothermal systems have clearly demonstrated that seawater circulates deep into sedimentary formations and also the underlying oceanic crust. For the Atlantis II Deep hydrothermal system, this means that seawater probably circulates right down to the magma chamber (Fig. 1), despite the low-permeability intervening sediments. According to our new geological model [4, 6], at least three zones of the Atlantis II Deep sub-seabed system possess the potential for being natural salt ‘factories’. The first of these are the warm brine pools on the seafloor, at a water depth of 2,100 m, where salt precipitates due to cooling. Then there are two zones in which salt precipitates due to boiling and transition to the supercritical state. These are the central reflux and the flanking recharge zones (Fig. 1).

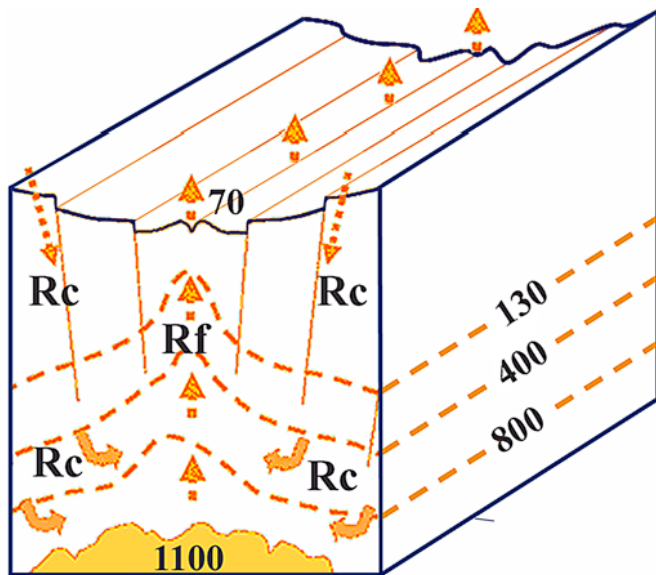


Fig. (1). A conceptual sketch (not to scale) illustrating our geological model. The sketch is drawn on the basis of inferred sub-surface conditions below the Atlantis II Deep, Red Sea [4, 8, 11]. Arrows indicate movement of fluids and particles, including molten and precipitating salts, brines, salt slurry (mush) and other mineral particles and gases. The magma chamber is shown at the bottom, with an indicated temperature of 1,100°C. R_c = Recharge zones. R_f = Reflux zone. The broken lines are isotherms at 130, 400, and 800 degrees C. The temperature at the seafloor is 70 degrees C, and at the magma chamber 1,100 degrees C. The seafloor is at a general depth of 2,100 m, and the magma chamber is located 1 km below seafloor. This 3D-model represents a rectangular section of the Atlantis II Deep which is 2 km wide, 10 km long, and where the depth to the magma chamber is 1 km below seabed surface.

The main driving force of the convective, circulatory fluid system is a very high temperature gradient caused by the shallow magma chamber (temperature range 900-1,200°C). Its depth is suspected to be 1 km below the seabed (~ 3 km below mean sea level) (Fig. 1), i.e. well within the supercritical P and T range for circulating seawater.

Basis for the Numerical Modeling

Observations from the Atlantis II Deep confirm the existence of ‘fountains’ occurring on the seafloor immediately above the magma chamber [13, 14, 15, 16, 17]. However, these fountains cannot continue to flow unless fluids are re-

charged into the system from the flanks of the rift. One such recharge source is the high-density brines in the seafloor brine-pools of the Atlantis II Deep. Because these brines are denser than normal seawater and because surface marine sediments are known to be of very high porosity, these brines probably sink down into the sediments, and migrate downwards along the flanks (Fig. 1). Inferred temperature distribution and circulation of fluids are indicated in the sketch (Fig. 1). According to Lewis and Holness [18], permeabilities of salt at depths of ~3 km may be similar to those of sandstones. Consequently, supersaturated brines will easily be transported through the buried salt formations. When such brines cool, salt particles are likely to crystallize.

The highest temperatures measured in the Red Sea brine-pools are $\leq 70^\circ\text{C}$ [13]. This means that brines entering into the seafloor under forced convection, will have to pass into higher and higher temperatures, $\leq 1,000^\circ\text{C}$, near the magma chamber. The following specific temperature zones are important in relation to salt formation:

- 130°C (the temperature where anhydrite in seawater becomes supersaturated),
- 430°C (the temperature where supercritical seawater precipitates NaCl at pressures > 300 bars),
- 800°C (the melting point for halite).

Description of our Modeled Hydrothermal System

Within the flanking recharge zones the down-going brines attain temperatures $>130^\circ\text{C}$ at shallow depth beneath the sediment surface. Here, the retrograde solubility of anhydrite causes super-saturation, and anhydrite precipitation (Fig. 1). However, the brines contain many other dissolved salts including sodium chloride which are prograde and which continue to move deeper in solution into warmer regions of the system.

When the brines migrate deeper than 2,800 m ($p=300$ bar) and attain temperatures $> 430^\circ\text{C}$, they are under supercritical conditions, where auto-precipitation of salts (mainly halite) occurs [4, 6]. This is the out-salting region where salts will accumulate in faults, fissures, and fractures. However, the low-density supercritical water vapor will migrate vertically upwards out of the system. At depths shallower than 2,800 m the water vapor becomes sub-critical, and condenses [19]. This condensation water is more buoyant than the surrounding brines and may even reach right up to the seafloor without being able to re-dissolve much salt.

The flow of water through this zone will tend to re-dissolve the accumulated salt and transport it upwards. This dissolution/transportation process also involves a refining of the various salts according to their solubility in hot water, e.g., magnesium chloride, which is much more soluble than sodium chloride, is preferably transported further out of the system than sodium chloride.

The temperatures in the immediate vicinity of the magma chamber exceed 800°C , which is above the melting point of most relevant salts. Molten salts that migrate out of this zone will encounter and mix with supercritical water. This fluid also migrates vertically in the central reflux zone. Salt will precipitate due to cooling when passing into regions of pressure and temperature at which solubility limits are exceeded.

Saturated brines migrating upwards from the central re-flux zone will feed into the fountains on the seafloor and accumulate in the brine pools. When these cool down, halite and other salts precipitate [20].

Boundary Modeling Conditions

We modeled the Atlantis II Deep hydrothermal system by choosing a set of predicted boundary conditions and selecting the necessary physical and thermodynamic parameters as simple and realistic prerequisites, based on geophysical, drilling, and other published results, and from our geological model for the area [7, 8, 9, 10, 11, 12, 13, 14, 15, 16, 17, 19]. These were fed into the numerical 2D sedimentary basin model, combined with a numerical molecular model. The objectives of our simulations were to provide a first order approximation of how salts (mainly anhydrite and halite) affect the convection cell generated by the buried hot magma chamber. We used the following prerequisites:

- 1) Underneath the Atlantis II Deep there exists a 3-dimensional forced convection cell of circulating seawater and brine, driven by a shallow, strong heat-source [11,13,19].
- 2) The heat-source consists of a magma chamber, located 1 km sub-seabed (i.e., 3 km total depth below mean sea-level) [11, 13].
- 3) The upper zone of the magma chamber has a constant temperature of 1,100°C [17].

For modeling purposes, the additional constraints were (based on [9-19]) (Fig. 1):

- A. The intervening sediments located between the magma chamber and seafloor consists of a mixture of solid sediments, volcanics, and evaporites, i.e. salts. The inferred composition was: 50% anhydrite, 40% halite, and 10% volcanics and other rock debris.
- B. The size of the surface hydrothermal outflow is 10 km by 4 km, in a rectangular area located directly above the magma chamber.
- C. The upward directed brines flow out of the seafloor (within this area) at a flux rate of 2 m per year [10,19].
- D. Hydrothermal recharge of seawater occurs in zones located immediately outside this area.
- E. The recharging fluids originate from the water column, and are sourced equally from high-salinity brines located within the Atlantis II Deep (50%), and from normal seawater (50%).
- F. Because the water depth is < 2,800 m, the supercritical water will start to boil at some stage during vertical ascent, on passing out of the supercritical pressure regime.

We infer that the magma chamber does not cool down, despite that it is making contact with seawater. The reason is that the amount of water making this contact is very small compared to the size of the inferred magma chamber and over the small time-frame (hundreds of years) we have used in the simulation.

SIMULATION TECHNIQUES

Density, Enthalpy, and Viscosity of Brine

A model geothermal fluid was used to determine the properties of the hot brines of the Atlantis II Deep geothermal system above the magma chamber. We followed the approach of Palliser & McKibbin [21] in designing a system that approximated a pure NaCl—H₂O system without perfectly matching the data for the pure system; an exact equation of state for pure water was used when no salt was dissolved in the system (condensation water).

A reservoir simulation algorithm called 'ATHENA' (see notes) for multiphase flow in porous media was employed [22]. The primary variables for this program package are temperature, pressure and molar masses for each fluid and solid component. Required density, enthalpy and viscosity of all phases involved in heat and mass transport throughout the reservoir were calculated by implementing the correlation formulae for the gas, liquid and solid phases tabulated in Palliser and McKibbin [23, 24] and linking them with the original code.

The model system was treated as potentially consisting of two phases: fluid and solid. Within the fluid and solid salt coexistence regions [21], the maximum solubility of NaCl in either gas or liquid served as the "bubble-point" curve closely resembling its counterpart in case of gas-liquid equilibrium. Simulated lithologies included sandstone with a permeability of 3 mD and porosity of 0.35, and clay (permeability 0.01 mD, porosity 0.1025). These values were chosen as they are standard for reservoir simulations in the hydrocarbon industry, and also represent conservative values. The fluid flow took place in a two-phase system, with relative permeabilities and capillary pressures specified for each lithological type. The initial NaCl content of brine was assumed to be 5% molar throughout the formation [25, 26].

The pressure boundary conditions consisted of specified pressure at the top (22MPa [15]), hydrostatic pressure on the left- and right-hand sides, as well as absence of vertical fluid flow at the bottom. Temperatures were held fixed at 340 °K at the top [16] and 1,400 °K at the magma chamber top. These boundary conditions were supplemented by setting the heat flux to zero for the remaining part of the bottom and the left- and right-hand sides.

The reservoir geometry corresponds to the sketch in Fig. (1), with the area ranging 2,000 m in width, and 1,000 m depth (height). Because the model simulates a system that is very long (the Atlantis Deep system is 70 km long) compared to its width (4 km), the length in the y-direction is considered constant (2-D simulation). A uniform grid was used for the simulation, with cell size 25 m x 25 m. Both heat and fluid flow were considered two-dimensional. A 5 meter-thick clay layer with an opening of 25 m in the middle separated the magma chamber from the overlying sandstone and low-permeability sediment/crustal layers.

Because our first simulation resulted in a rather long time before the steady state situation was achieved (200 years), we tested the effect of having relief on the magma chamber. This test proved that a slight relief on the magma chamber, whereby it was intrusive into the sand, made the hydrothermal system become much more efficient. Two different

cases were therefore simulated: Case 1, with a 25 m wide opening between the magma chamber and the sand reservoir, referred to as ‘flat magma chamber opening’ case, and Case 2, which simulated a magma intrusion into the reservoir, with an 80 m high magma body protruding into the sand reservoir, where the hot magma body was sheathed (insulated) by a 25 m thick clay layer. This scenario is referred to as ‘intrusive magma chamber’ case.

RESULTS AND DISCUSSION

Case 1: Flat Magma Chamber Opening

The numerical simulation calculated the evolution of the described system over a period of 200 years, after which, the system reached a steady state. We observed both the appearance and disappearance of the solid salt phase (outsalting and re-dissolution). It was previously taken for granted that outsalting significantly lowered the porosity and permeability of the cells. This meant that affected cells would experience decreasing permeability. However, in view of the experimental evidence [18, 27] that rock salt attains high permeability under similar pressure and temperature conditions, we assumed that neither outsalting nor re-dissolution affected the permeability of the cells.

The steady-state distribution of temperatures after a 200 year simulation run is depicted in Fig. (2a). The temperature behaves as predicted, without detectable anomalies. Fig. (2b) shows the corresponding steady-state hydrothermal circulation that developed. Arrows point in the direction of the Darcy flow, with the arrow length reflecting the flow speed. The different colors only represent different initial building blocks and have no physical meaning. As seen in this figure, our system features a well-defined and predicted flow pattern. Of especial interest are the recharge zones (the downward flow at the sides), as well as vigorous upward flux above the magma chamber. Thus our simulation manages to reproduce relevant circulation phenomena without the need of placing any artificial flux constraints beyond the boundary conditions.

Assessing the effects of the salt precipitation caused by either subcritical boiling or supercritical outsalting was one of the goals of the present study. As discussed previously, the realistic brine thermodynamics we implemented will make a second (solid) phase to appear in the system under certain temperature and pressure conditions. After 200 years, the Atlantis II simulation develops a dome-shaped region with a high concentration of precipitated salt. This “dome” can be clearly seen in Fig. (2c); it measures ~100 meters in height and 250 meters at the base, and although the molar fraction of the solid salt within the dome ranges ~ 8%, its sheer size translates into huge volumes of salt. Even if the precipitate mostly consists of sodium chloride, the concentration of rare-metal salts (whose thermodynamics closely mimics those of common salts) is notably higher than found, for instance, in the original seawater.

Case 2: Intrusive Magma Chamber

The second scenario involved simulating a sill intrusion from the magma chamber consisting of an 80-meter high and 25-meters wide magma region with zero permeability and zero porosity, and insulated from the above sediments by a 25-meters thick clay layer. The steady-state distribution of

temperatures was now achieved already after a 50 year simulation run (Fig. 3a). Again, the temperature behavior seems to be quite realistic, with the presence of an upward-pointing heat-flow. On the other hand, modifications made to the heat source geometry have notably changed the steady-state hydrothermal flow pattern, shown in Fig. (3b). For example, the Darcy flow in the central area has now become much more vigorous than in the previous scenario (compare the length of arrows in Figs. (2b,3b)). Another difference is a somewhat more complicated flow pattern. Note the clear-cut recharge zones, and that the system still successfully reproduces our predicted convective circulation pattern.

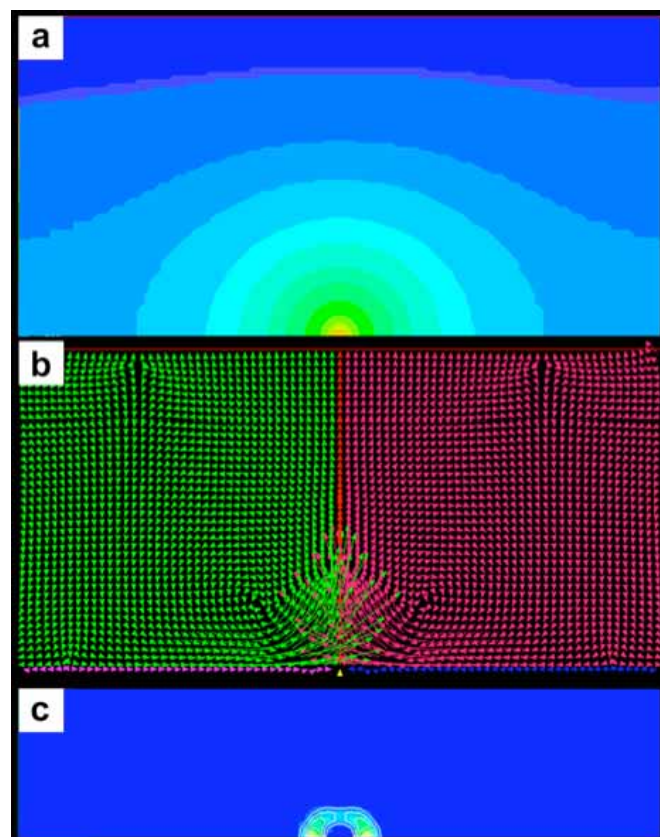


Fig. (2). Numerical simulation and modeling results, Case 1 (flat magma chamber opening) after 200 years.

- a) Steady-state temperature distribution. Red colour indicates a temperature of 1,400 K; blue, 340 K. The dimensions of this 2D-model, is 2 km in width and 1 km in depth.
- b) Steady-state Darcy flow pattern of the same case. Arrows indicate the direction of the Darcy flow; arrow length reflects the flow speed. The same dimensions have been used as in a).
- c) Steady-state solid salt content (molar fraction) of the same case. The same dimensions have been used as in a). See text for details and discussion.

Fig. (3c) shows the dramatic effect of changing the heat source geometry on salt precipitation. The steady-state distribution of solid salt content has tripled in height and more than doubled in width at the base. But, the salt content is just one fifth of the previous (Case 1) scenario. This means that even though the total volume of precipitated salts has increased significantly, the whole amount is spread over a much larger area (volume) compared to the scenario in Case

1. This is probably an effect of a much more dynamic convective system.

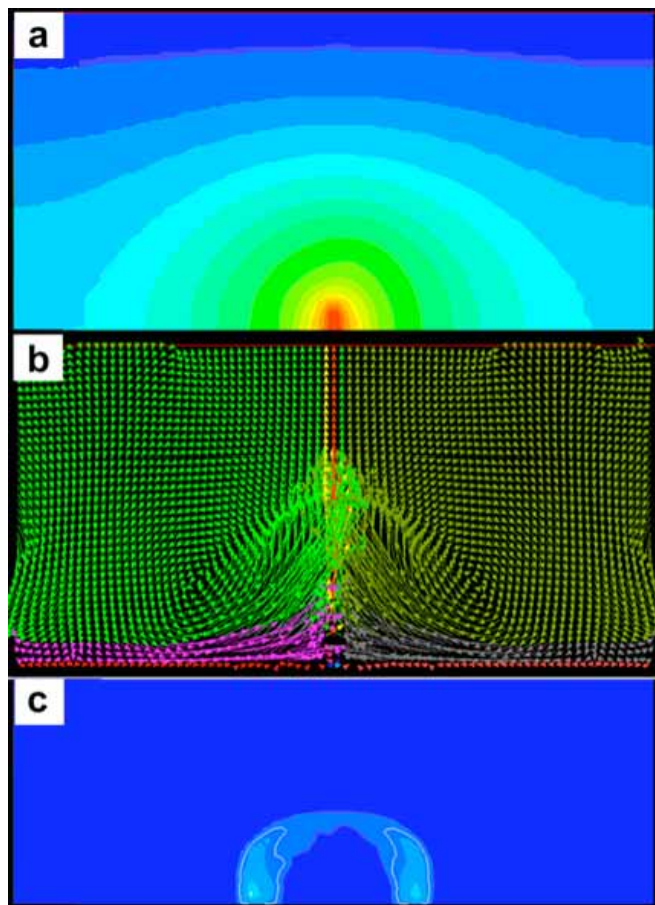


Fig. (3). Numerical simulation and modeling results, Case 2 (the magma intrusion) after 50 years.

- Steady-state temperature distribution. Red colour indicates a temperature of 1,400 K; blue, 340 K. The dimensions of this 2D-model, is 2 km in width and 1 km in depth.
- Steady-state Darcy flow pattern for the same case. Arrows indicate the direction of the Darcy flow; arrow length reflects the flow speed. The same dimensions have been used as in a).
- Steady-state solid salt content (molar fraction) for the same case. The same dimensions have been used as in a). See text for details and discussion.

CONCLUSIONS

Laboratory experiments and theoretical considerations have demonstrated that supercritical water has extremely low solubility for normal sea salts. The fact that solid salts precipitate from seawater in its supercritical state suggests the possibility that seawater circulating in faults and fractures near underground heat sources may precipitate large amounts of salts. For a theoretical examination of this concept, we selected the Atlantis II Deep hydrothermal system in the Red Sea.

By implementing the Palliser-McKibbin model [21], for deep geothermal brines within the reservoir simulation algorithm ATHENA, we modeled a hydrothermal out-salting system analogous to that observed in the Red Sea. With the initial setup and boundary conditions corresponding to a hot magma chamber located 1 km beneath the Atlantis II Deep,

our simulations show that phase changes brought about by temperature and pressure variations, produce large-scale depositions of salt in a dome-shaped bodies. Our simulations show that the size and salt contents of such domes vary according to magma (intrusive) geometry. The domes can range from 150 m to several hundred meters in height and width, depending on the magma geometry. The numerically modeled brine flow patterns closely resembled our hypothesized picture of recharge and reflux zones. Thus, in addition to confirming our general prediction of the Atlantis II Deep hydrothermal out-salting, the numerical simulation results also show that there probably exists a focused upward reflux zone on the seafloor immediately above the apex of the magma chamber. This explains the existence of hot-brine ‘geysers’ observed in the Atlantis II Deep. Our model shows that the effects of tectonically induced and hydrothermally-associated salt production and accumulation are much more complex and probably more widespread than previously realized.

ACKNOWLEDGEMENTS

We gratefully acknowledge the help of Dr Christopher Palliser who has kindly supplied the FORTRAN version of the code that enables to delineate the T-p-X space and calculate critical and saturation curves for brine, H₂O, and NaCl, the mass fractions of halite in saturated water vapor and liquid, as well as the equation of state for pure water. We thank Christian Hensen, Claus Wallmann, and David Turnbull for fruitful discussions and Statoil ASA for releasing this information for publication.

NOTES

‘ATHENA’

Control-volume finite-difference space discretization together with a backward Euler scheme is used for time discretization of pressure and temperature equation and a sequential implicit solver for the balance equations. Both conductive and convective heat exchanges are accounted for. The missing solid phase data was fixed by matching the NaCl enthalpy values from Archer [25] to the saturated liquid data for salt [24] at the sodium chloride melting point (800°C, heat of fusion 30.23 kJ/mole).

Quasi-single phase fluid was used to reproduce the brine properties in the liquid-gas co-existence region (region 5). Analytical “flash” calculations (combined mass balance and phase equilibrium calculations) were performed in the two-phase gas-liquid region to determine the liquid fraction of the fluid mixture and subsequently the net density and enthalpy [23, 24]. The correlations of Palliser & McKibbin [23] provided the liquid and the gas fractions and corresponding equilibrium distribution conditions. Temperature, pressure and concentration dependence of brine’s dynamic viscosity was calculated from the correlations formulae tabulated in Palliser & McKibbin [24, 26]. As in the case of densities and specific enthalpies, the viscosities were used as input for the ATHENA reservoir simulator described in the next section. Solid-state NaCl properties not covered by the original model were estimated by combining data from several other recent sources. To replace a two-phase liquid gas mixture with an appropriate single-phase fluid, analytical flash calculations were used.

REFERENCES

- [1] F. J. Armellini, "Phase equilibria and precipitation phenomena of sodium chloride and sodium sulphate in sub- and supercritical water", Ph. D Thesis, Massachusetts Institute of Technology, Cambridge, Massachusetts, USA, Feb. 1993.
- [2] J. Tester *et al.*, "Supercritical water oxidation technology", In: D. W. Tedder, F. G. Pohland, Ed., *Emerging technologies in hazardous waste management III*, American Chemical Society; pp. 35-76, Aug. 1993.
- [3] M. Hodes, P. Griffiths, K. A. Smith, W. S. Hurst, W. J. Bowers, K. Sako, "Salt solubility and deposition in high temperature and pressure aqueous solutions", *Aiche J*, vol. 50, no. 9, pp. 2038-2049, Sept. 2004.
- [4] M. Hovland *et al.*, "Sub-surface precipitation of salts in supercritical seawater", *Basin Research*, vol. 18, pp. 221-230, Feb. 2006.
- [5] N. Lmmen, B. Kvamme, "Kinetics of NaCl nucleation in supercritical water investigated by molecular dynamics simulations", *Phys Chem Chem Phys*, vol. 9, pp. 3251-3260, Dec. 2007.
- [6] M. Hovland, H. G. Ruesltten, H. K. Johnsen, B. Kvamme, T. Kutznetsova, "Salt formation by supercritical seawater and submerged boiling", *Mar Petrol Geol*, vol. 23, pp. 855-869, Dec. 2006.
- [7] E. T. Degens, D. A. Ross, "Hot brines and recent heavy metal deposits in the Red Sea", New York; Springer Verlag, pp. 535-541, Mar. 1969.
- [8] J. D. Lowell, G. J. Genik, "Sea-floor spreading and structural evolution of southern Red Sea", *Am Assoc Petrol Geologists Bull*, vol. 56, pp. 247-259, Feb. 1972.
- [9] E. Savoyat, A. Shiferaw, T. Balcha, "Petroleum exploration in the Ethiopian Red Sea", *J Petrol Geol*, vol. 12, pp. 187-204, Feb. 1989.
- [10] C. Ramboz, E. Oudin, Y. Thisse, "Geyser-type discharge in Atlantis II Deep, Red Sea: Evidence of boiling from fluid inclusions in epigenetic anhydrite", *Can Mineral*, vol. 26, pp. 765-786, Mar. 1988.
- [11] R. B. Whitmarsh, P. E. Weser, D. A. Ross, *Initial reports of the Deep Sea Drilling Project*, U.S. Government Printing Office, Washington, vol. 23, pp. 821-847, Jun. 1974.
- [12] F. Orszag-Sperber, G. Harwood, A. Kendall, B. H. Purser, "A review of the evaporites of the Red Sea – Gulf of Suez rift", In: B. H. Purser, D. W. J. Bosence, Ed, *Sedimentation and tectonics of rift basins: Red Sea – Gulf of Aden*, London, Chapman & Hall, pp. 409-426, May 1998.
- [13] R. A. Zierenberg, M. E. Holland, "Sedimented ridges as a laboratory for exploring the subsurface biosphere", In: W. S. D. Wilcock, E. F. DeLong, D. S. Kelley, J. A. Baross, S. C. Cary, Ed, *The sub-seafloor biosphere at mid-ocean ridges*, American Geophys. Union, pp. 305-323, Apr. 2004.
- [14] E. Faber, R. Botz, J. Poggenburg, M. Schmidt, P. Stoffers, M. Hartmann, "Methane in Red Sea brines", *Org Geochem*, vol. 29, pp. 363-379, Jan. 1998.
- [15] M. Hartmann, J. C. Scholten, P. Stoffers, F. Wehner, "Hydrographic structure of brine-filled deeps in the Red Sea – new results from the Shaban, Kebrit, Atlantis II, and Discovery Deep", *Mar Geol*, vol. 144, pp. 311-330, Jul. 1998.
- [16] M. Hartmann, J. C. Scholten, P. Stoffers, "Hydrographic structure of brine-filled deeps in the Red Sea: correction of Atlantis II Deep temperatures", *Mar Geol*, vol. 144, pp. 331-332, Nov. 1998.
- [17] G. R. McMurray, Ed, *Gorda Ridge: A seafloor spreading center in the United States Exclusive Economic Zone*, New York, Springer-Verlag, Sep. 1990.
- [18] S. Lewis, M. Holness, "Equilibrium halite-H₂O dihedral angles: High rock-salt permeability in the shallow crust?" *Geology*, vol. 24, pp. 432-434, May 1996.
- [19] G. Winckler, *et al.*, "Sub sea floor boiling of Red Sea brines: New indication from noble gas data", *Geochim Cosmochim Acta*, vol. 64, no. 9, pp. 1567-1575, Oct. 2000.
- [20] B. C. Schreiber, "Subaqueous evaporite deposition", In: B. C. Schreiber, Ed, *Evaporites and hydrocarbons*, New York, Columbia Univ Press, 182-255, Dec. 1988.
- [21] C. Palliser, R. McKibbin, "A model for deep geothermal brines, I: T-p-X state-space description", *Transport in Porous Media*, vol. 33, pp. 65-80, Feb. 1997.
- [22] I. Garrido, G. E. Fladmark, M. Espedal, "An improved numerical simulator for multiphase flow in porous media", *Int J Num Meth Fluids*, vol. 44, pp. 447-461, Dec. 2004.
- [23] C. Palliser, R. McKibbin, "A model for deep geothermal brines, II: Thermodynamic properties – Density", *Transport in Porous Media*, vol. 33, pp. 129-154, Feb. 1998.
- [24] C. Palliser, R. McKibbin, "A model for deep geothermal brines, III: Thermodynamic properties – Enthalpy and viscosity", *Transport in Porous Media*, vol. 33, pp. 155-171, Mar. 1998.
- [25] D. G. Archer, "Enthalpy increment measurements for NaCl(cr) and KBr(cr) from 4.5 K to 350 K. Thermodynamic properties of the NaCl+H₂O system", *J Chem Engineer Data*, vol. 42, pp. 281-292, Feb. 1997.
- [26] D. W. Kaufmann, "Sodium chloride the production and properties of salt and brine", *Am Chem Soc Monogr Ser*, no. 145, New York, Hafner Publ Comp, Aug. 1968.
- [27] M. B. Holness, S. Lewis, "The structure of halite-brine interface inferred from pressure and temperature variations of equilibrium dihedral angles in the halite-H₂O-CO₂ system" *Geochim Cosmochim Acta*, vol. 61, no. 4, 795-804, Mar. 1997.